# Analysis of Switching Transients of an EHV Transmission Line Consisting of Mixed Power Cable and Overhead Line Sections

M. Kizilcay, K. Teichmann, S. Papenheim, P. Malicki

*Abstract* -- **Within the scope of transmission system expansion plan of Germany new EHV transmission lines will be mixed lines consisting of several cable and overhead (OHL) line sections. Because of significantly higher charging current of XLPE cables it is necessary to install shunt reactors along those mixed lines that will be switched together with the line. A planned double-circuit 380-kV transmission line with total length of 180 km is of interest for the analysis of switching and fault transients in this paper, where four cable sections have a total length of 15 km.**

*Index Terms* – **Compensation, mixed line, EHV cable, shunt reactor.**

## I. Introduction

Erection of new EHV transmission lines in Germany are prescribed by law passed in 2009 in order to realize transmission grid expansion that will enable to transport electrical power generated by large off-shore wind farms in North to the South until 2020 [1]. In addition, the Act of Federal Requirements Plan that came in 2015 into effect establishes the need for energy efficiency and to ensure a safe and reliable grid operation for the decided projects. According to both measures approximately 8000 km new transmission lines have been decided to erect in Germany. It is a good compromise to build parts of those transmission lines as underground cables, specially, in the urban areas. As a consequence new 380-kV transmission lines will be mixed lines consisting of several cable and overhead line (OHL) sections. However, the predominant length of the lines will be erected as overhead line.

Because of significant high capacitive charging current of power cables it is necessary to install shunt reactors along those mixed lines that will be switched together with the transmission line [2]. The shunt reactor as a nonlinear element interacts with the transmission line by electromagnetic transients initiated by switching and fault surges.

A planned double-circuit 380-kV transmission line with total length 180 km is of interest for the analysis of switching and fault transients. The line consists of four cable sections with a total length of 15 km and five OHL sections with a total length of 165 km. The inductive shunt compensation will vary between 50 and 250 MVAr for each circuit by installing two shunt reactors on the line. This varying compensation requirement has been determined by steady-state power flow computations and is not within the scope of this paper. This paper deals with the transient analysis of various switching and fault phenomena on that double-circuit transmission line. Digital simulations of electromagnetic transients have been carried out using EMTP-ATP software [3]. The simplified configuration of the line with OHL and cable section lengths in km is shown in Fig. 1. Further EHV mixed lines with higher proportion of cable section lengths will be studied in future.

The paper is structured as follows: System data and simulation models of the components are described in section II. Results of various simulations are presented and discussed in section III. Finally, important conclusions are summarized in section IV.

## II. System Data and Simulation Model

### A. Source Network Equivalents

The 380-kV grid connected in substations (S/S) A and B (Fig. 1) is represented by a simplified Thevenin equivalent using available positive- and zero-sequence short-circuit impedances based on short-circuit data given in TABLE I. The line-to-line voltage behind the three-phase short-circuit impedance is selected as 400 kV.

TABLE I
Short-Circuit Data to Represent Network Equivalents

| | **Substation A** | **Substation B** |
|---|---|---|
| Max. short-circuit power (GVA) | 42.8 | 25.5 |
| Min. short-circuit power (GVA) | 15 | 6.2 |
| $Z_{zero\text{-}seq.}$ / $Z_{pos\text{-}seq.}$ (ratio) | 1.66 | 2.78 |
| $R_{pos\text{-}seq.}$ / $X_{pos\text{-}seq.}$ ≈ $R_{zero\text{-}seq.}$ / $X_{zero\text{-}seq.}$ | 0.1 | 0.1 |

M. Kizilcay, K. Teichmann, S. Papenheim and P. Malicki are with the Dept. of Electrical Eng. and Computer Science of the University of Siegen in Siegen, Germany. (e-mail of corresponding author: kizilcay@uni-siegen.de).

Paper submitted to the International Conference on Power Systems Transients (IPST2017) in Seoul, Republic of Korea June 26-29, 2017

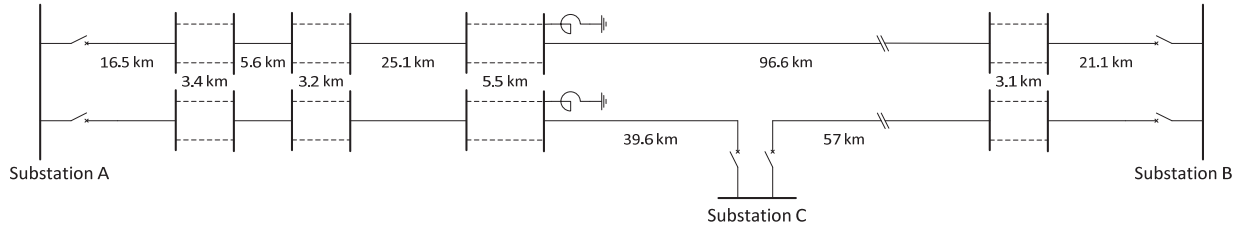


Fig. 1. Configuration of the 380-kV mixed double-circuit line with OHL (——) and cable sections (------)

### B. *Overhead Line Sections*

Typical tower layout for the double-circuit line is shown in Fig. 3. Conductor type and electrical data of the major OHL sections are given in TABLE II. OHL sections shown in Fig. 1 in fact consist of several shorter subsections with various tower layouts and number of circuits. They are represented by "Constant-Parameter Distributed Line" (CPDL) model [3]. Line parameters are calculated at $f = 200$ Hz, which has been determined based on the resonant frequency of the whole line.

TABLE II
OHL CONDUCTOR TYPE AND ELECTRICAL PARAMETERS

| | |
|---|---|
| Phase conductor | 4 x 550/70 ACSR |
| Ground wire | 1 x 550/70 ACSR |
| Positive-sequence impedance | (0.013 + j0.249) Ω/km |
| Positive-sequence capacitance | 14.275 nF/km |
| Zero-sequence impedance | (0.094 + j0.891) Ω/km |
| Zero-sequence capacitance | 6.54 nF/km |

### C. *Cable Sections*

The four cable sections indicated in Fig. 1 consist of two XLPE cables per phase and will be buried in ground. Hence for the 380-kV double-circuit line total 12 XLPE cables (four circuits) are installed in each section as shown in Fig. 2. Cables are single-core (SC) XLPE cables of the type 2XS(FL)2Y 1x2500 RMS/250 220/380 kV. The screens of the cable circuits are cross-bonded; each cable system is subdivided into 3 or 6 cross-bonding sections depending on the cable length.

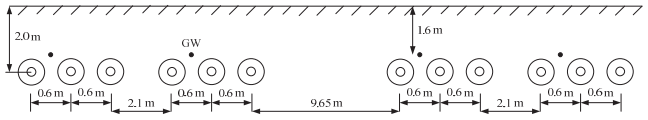


Fig. 2. Layout of cable sections

Metal-oxide surge arresters are taken into consideration at the cross-bonding locations across the sheath and ground. The CABLE PARAMETERS (CP) routine [3] of EMTP-ATP is used to create basic electrical parameters of the cable. CP produces directly model data for CPDL model and for a multi-conductor Pi-circuit.

### D. *Shunt Reactor*

The 400-kV shunt reactor (SR) as a three-phase unit is located at the right terminal of the 5.5 km long cable section (see Fig. 1). The neutral point is grounded solidly. The reactive power hence the reactance can be varied in the range of 50..250 MVAr by means of an on-load tap changer. The design parameters are as follows:

- rated power: 250 MVA; rated voltage: 400 kV
- load losses: 420 kW; winding resistance at 75° C: 770 mΩ

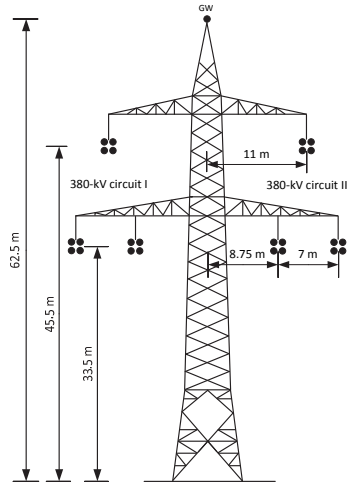


Fig. 3. Typical 380-kV OHL tower

From the magnetizing characteristic given for 250 MVAr, the magnetizing curves for different settings have been estimated by taking number of turns of the winding at different tap changer positions into consideration. Fig. 4 shows linked magnetic flux vs. current characteristics for the settings 50, 125 and 250 MVAr.

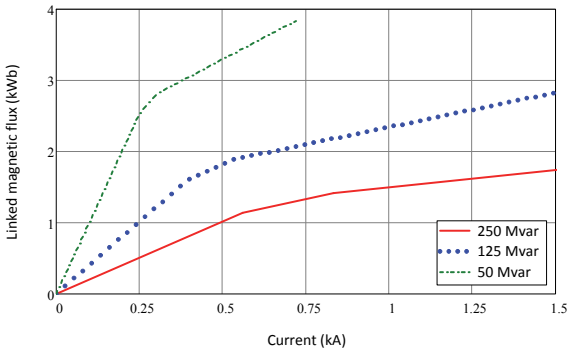


Fig. 4. Current-flux characteristics of the shunt reactor

### E. *Line Surge Arresters*

Surge arresters of MOV type are needed at each junction of an OHL and cable section in order to protect the cable against lightning surges. Metal-oxide surge arresters with $U_r = 336$ kV are proposed by the TSO. They are represented using the simplified IEEE model [4]-[5] by two non-linear resistors $A_0$ and $A_1$ for the slow and fast surges. The equivalent circuit of the surge arrester is shown in Fig. 5. The inductances $L_0$ and $L_1$ are calculated according to [5], [6].

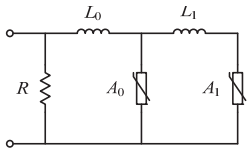


$L_0$ = 1.68 µH
$L_1$ = 5.04 µH
$R$ = 100 MΩ

Fig. 5. Surge arrester model

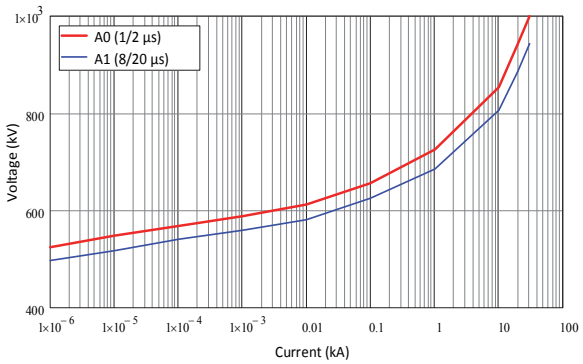


Fig. 6. Voltage-current characteristic of line surge arrester

The voltage-current characteristic of the surge arrester is shown in Fig. 6.

### F. *Voltage Transformers*

Inductive voltage transformers (VT) will be installed at the location of shunt reactors and at both line ends (line side) that will be switched off together with the line. Total three VT sets will be connected at line side for the upper circuit in Fig. 1. Depending on the compensation degree or at worst case without shunt compensation the VT's may be stressed due to the capacitive charging power of the cable and OHL sections, when the line is disconnected. The data and model of the 420-kV SF6 voltage transformer are taken from [16]. Following data are used to model linear part of the VT.

- Voltage ratio: 4000
- Winding resistance: HV: 20780 Ω; LV: 22 mΩ
- Leakage inductance: HV: 2290 H; LV: 31.9 µH
- Core losses (simplified): 1.54 GΩ (referred to HV).

The magnetizing curve referred to the HV side is given in Fig. 7. The core losses are represented alternatively by a ladder network shown in Fig. 8.

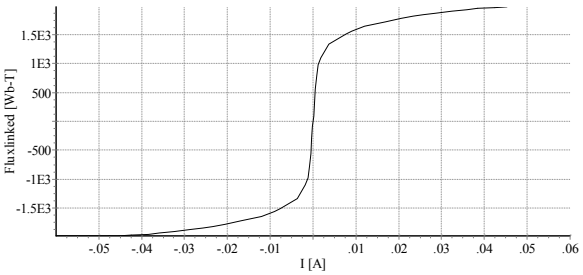


Fig. 7: Magnetizing curve of the VT

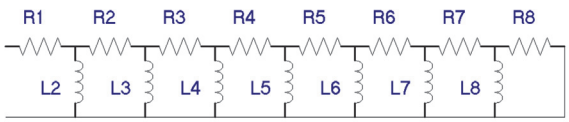


Fig. 8: Detailed representation of core losses

## III. Results of Studied Cases

### A. *Preliminary Considerations*

The 380-kV mixed line with several cable sections and shunt compensation may reveal different behavior compared to conventional OHL by considering following points.

- The maximum degree of compensation with the 250-MVAr shunt reactor amounts to 47.3 % for the upper circuit between S/S A and S/S B. The maximum compensation degree of 78.5 % is expected for the lower circuit between S/S A and S/S C (see Fig. 1).
- High capacitive charging current of cable sections may influence circuit breaker (CB) operation and secondary arc extinction, when single-pole autoreclosure (SPAR) is applied [7].
- Interaction with the non-linear SR connected to the line may cause overvoltages due to resonances. Since the reactance of the shunt reactor will vary according to the compensation requirement, it will be complicated to identify possible resonances and their impact [8], [9], [10].
- Surge arresters are required at each OHL-cable junction along the line to protect the cable section against lightning overvoltages.
- Circuit breakers will be installed at both line ends in substations A and B for the upper circuit (see Fig. 1). Hence the complete line will be switched on/off together with the shunt reactor. Depending on the switching instant, for example at voltage zero crossing, the switching current zero-crossing may be delayed due to shunt reactor interaction [9], [11], [12].
- Impact on inductive VT during de-energization of the line at different compensation levels of the shunt reactor.

In the light of these facts following phenomena have been studied by means of EMTP-ATP simulations:

- Energization of the transmission line at different degrees of shunt compensation;
- Influence of the short circuit power of source networks on line energization;
- Energization of the line at source voltage zero crossing and analysis of delayed zero crossing of line currents;
- Statistical analysis of line energization taking in consideration of CB pole spread;
- De-energization of the line at different degrees of shunt compensation including the case without compensation for different loading conditions with the purpose of analyzing transient recovery voltage of CB poles and examination of the stress on VT's;
- Analysis of single-pole autoreclosure (SPAR) by means of a dynamic fault arc model and determination of arc duration for different degrees of shunt compensation.

### B. *Line Energization*

At first step the influence of the shunt reactor on line energization has been studied. One circuit of the 380-kV line that is open at the receiving end has been energized alternatively from substations A and B, while the second circuit is disconnected. Switching cases with and without shunt reactor (compensation level 250 MVAr) in the energized circuit are computed. It has been observed that the switching voltage waveforms at the open end are marginally affected by the shunt reactor in the

first two periods of power frequency. Similar behavior is expected for current waveforms of the energizing CB. The simulation results of the energization case are shown in Fig. 9 and Fig. 10 taking following conditions into consideration:

- simultaneous closing of CB poles at phase A voltage peak;
- Energization from S/S A with max. short-circuit power;
- without and with the shunt reactor (250-MVAr setting)

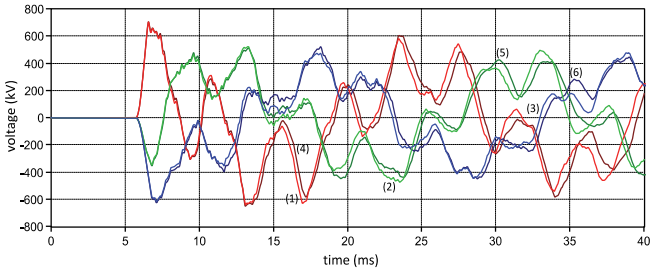


Fig. 9. Line-to-ground voltages at the open end of the line
(1), (2), (3) - with shunt reactor; (4), (5), (6) - without shunt reactor

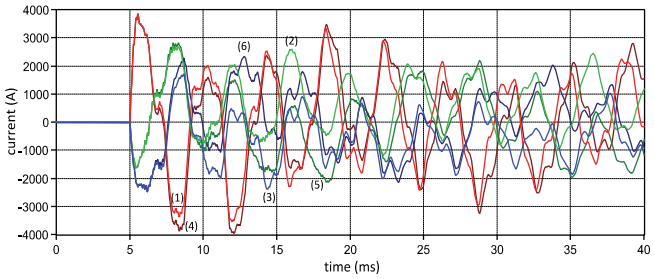


Fig. 10. Current of closing circuit breaker poles
(1), (2), (3) - with shunt reactor; (4), (5), (6) - without shunt reactor

As a complementing study, it is interesting to analyze the frequency scan of the driving-point admittance of the concerning line and source network in substation A, where the line is open at the receiving end (substation B). Frequency scan has been performed in a range of 10 Hz to 1.2 kHz. Influence of the shunt reactor on frequency response is studied for the cases: no SR, SR with 50 MVAr and 250 MVAr settings. SR is represented as linear component in a frequency scan computation [2]. Additionally, the influence of the short-circuit power (min. and max.) of the source network in substation A is taken into consideration.

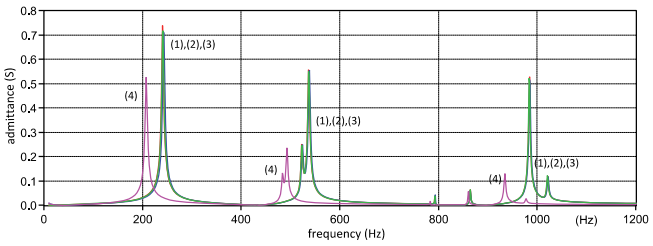


Fig. 11. Driving-point admittance of the open-end line (one circuit)
(1),(2),(3) – max. short-circuit power of source network
Cases: (1) – no SR; (2) – 50-MVAr SR; (3) – 250-MVAr SR
(4) – min. short-circuit power of source network

The computed magnitude of driving-point admittance for those cases is shown in Fig. 11. The influence of the SR on the resonant frequencies, for example in line current, is insignificant, whereas the short-short impedance of the source network has a higher effect. This frequency-domain analysis confirms the close similarity of energization transients with and without SR. In a time-domain simulation the non-linear inductance of the SR takes effect, however.

Another phenomenon experienced with shunt compensated lines is the delay of CB current zero-crossing depending on the closing instant of CB poles, when the line will be energized [11]. The worst-case occurs, if compensation level is high and the CB poles close at the instant of voltage zero-crossing, so that max. DC component in current is achieved. The lower circuit with 250-MVAr shunt compensation is energized from both ends in substations A and C separately. Each CB pole is controlled to close at the zero-crossing of the associated line-to-ground voltage. The largest delay current zero-crossing is expected, when the line is energized from S/S A with the max. short-circuit power of the source network at this substation, whereas the CB at S/S C is open. The CB pole currents with critical zero-crossing delay are shown for this case in Fig. 12. A suitable countermeasure to avoid controlled switching is to equip the CB with pre-insertion resistors (400 Ω).

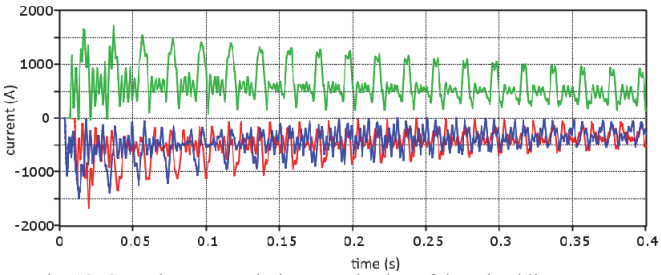


Fig. 12. CB pole currents during energization of the mixed line at zero-crossing of phase voltages

Statistical analysis of the energization overvoltages has been performed using statistical switch feature of [3]. The energization case is executed 200 times with uniformly distributed CB pole closing times in order to present cumulative frequency distribution of overvoltages at the receiving end of the mixed line. Overvoltages at the open receiving end and overcurrents of closing CB poles are the focus of attention. The difference in statistical distribution of overvoltages and CB overcurrents is minor with regard to the substation, from which the line is energized. The overvoltages are scaled by the overvoltage factor $k$ defined as

$$k = \frac{|v_{peak}|}{\frac{\sqrt{2}\cdot 380\ \text{kV}}{\sqrt{3}}} = \frac{|v_{peak}|}{310.27\ \text{kV}} \qquad (1)$$

The maximum overvoltage factor $k = 2.25$ expected at the open end of the line is relatively low due to limitation of switching overvoltages by the surge arrester sets located at each OHL-cable junction. Total 24 (3x8) surge arresters will be installed along each circuit of the transmission line. Energy absorbed by surge arresters during switching transients is not critical. Surge arresters are not equally stressed. The arrester set farthest from the substation, from which the line is energized, is more stressed than the other line surge arresters.

Corresponding cumulative frequency distributions for the overcurrents of the closing CB poles are presented in Fig. 13. According to Fig. 13 the maximum current peak expected is less than 5.5 kA and is independent of the shunt compensation. However, the probability of occurrence of overcurrents is lower, when the shunt reactor is in service.

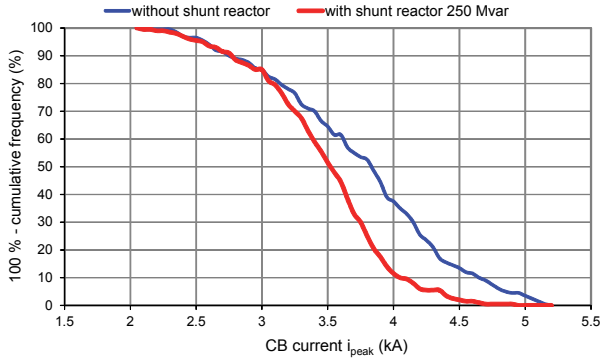


Fig. 13. Cumulative frequency distributions of overcurrents of closing CB

### C. *Single-Phase Autoreclosure Performance*

During SPAR of the faulted circuit extinction behavior of secondary arc should be investigated. Primary arc is effective after fault inception until single-phase tripping of the faulty phase. Secondary arc follows the primary arc after isolating the fault by single phase tripping at both ends. The transient interaction of the arc with the shunt compensated line can be investigated by a dynamic arc model [13], [14]. Following factors for the mixed line are investigated.

- fault location
- compensation level
- different phase conductors on tower

The arc model used in this work is based on the energy balance of the arc column and describes an arc in air by a differential equation of the arc conductance $g$ [14]:

$$\frac{dg}{dt} = \frac{1}{\tau}(G - g) \qquad (2)$$

where

$\tau$ : arc time constant,
$g$ : instantaneous arc conductance,
$G$ : stationary arc conductance.

Derivation of these parameters and details of arc modelling in EMTP-ATP are provided in [14]. The length of the primary arc is considered to be constant. A linear time-varying elongation of the secondary arc is taken into account by the model. In reality the arc length variation is highly dependent on external factors like wind, thermal buoyancy. The arc time constant $\tau$ is assumed to be constant during the primary arc. The time constant of the secondary arc is time-varying and can be expresses as a function of arc elongation [14].

The arc extinction phenomenon is not known in detail. The arc extinction in this study is based on thermal instability of arc described using (3). The arc extinguishes, if the time derivative of instantaneous arc resistance, $dr'/dt$, exceeds a pre-defined limit provided arc conductance $g'$ per length is less than a certain value. The following limiting values per arc length are determined empirically:

$$g'_{\min} = 50\,\mu\mathrm{S}\cdot\mathrm{m};\ \frac{dr'}{dt} = 20\,\mathrm{M\Omega}/(\mathrm{s}\cdot\mathrm{m}) \qquad (3)$$

During interruption of the faulty phase with arc fault, voltage from the sound phases of the double-circuit line is coupled to the faulty phase by capacitive and inductive coupling.

As the arc elongates the arc voltage increases with the arc length. When the arc voltage is in the range of coupled voltage from sound phases without arc, the arc becomes unstable. Therefore, it is important to determine the steady-state coupled voltage to the concerning phase without fault, but disconnected at both ends.

The results of steady-state computation of coupled voltages (rms value) to each phase conductor of the lower circuit between S/S A and C as worst case are summarized in Fig. 14 depending on line loading (real power transmission per circuit 700 MW and 1400 MW from S/S C to A) and compensation level (125 MVAr and 250 MVAr). The largest coupled voltages are expected in phase C for power transmission of 1400 MW and shunt compensation of 250 MVAr for each circuit. Consequently, arc duration during SPAR is expected to be longest in that phase. The shortest arc duration is expected for the shunt reactor out of service (without compensation).

Coupled voltages are rather of capacitive type. Shunt reactor is connected parallel to phase-to-earth line capacitance (see Fig. 15). Thus coupled phase-to-ground voltage will be higher with the shunt reactor based on voltage division due to higher impedance between phase 1 and ground. Power flow direction was assumed to be from S/S C to S/S A. Thus coupled voltage at sending end in S/S C is slightly higher.

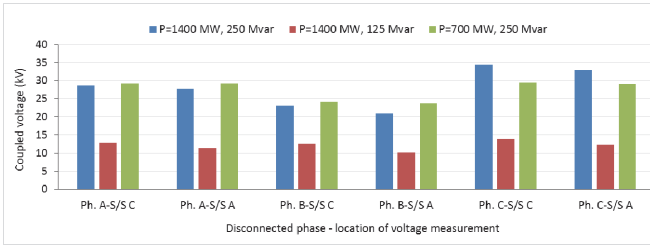


Fig. 14. Coupled phase-to-ground voltages to each disconnected phase

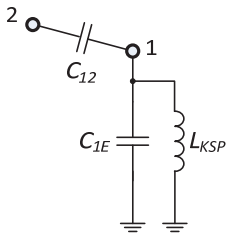


Fig. 15. Voltage divider with disconnected phase 1 and sound phase 2

The longest secondary arc duration for a conservative arc elongation speed (arc reaches 10 times of its original length in 1 s) is expected to be 1.3 s and occurs in phase C for line loading with 1400 MW and shunt reactor with 250 MVAr. The computed waveforms of secondary arc voltage and current with subsequent arc extinction are presented in Fig. 16. Arc fault occurs at $t$ = 12.4 ms and the faulty phase C is disconnected at both ends at $t$ = 97 ms. Finally arc extinguishes at $t$ = 1.39 s.

### D. *Line De-energization*

The de-energization of the mixed line is studied for different shunt compensation levels l50 MVAr, 125 MVAr and 250 MVAr per circuit. After de-energization of one circuit the phase voltages of the disconnected circuit oscillates with the

frequencies between 18 and 38 Hz depending on compensation level.

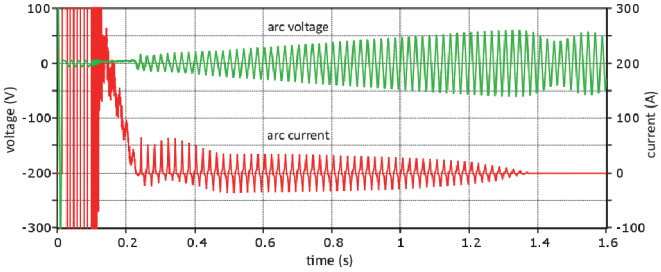


Fig. 16. Arc voltage and current

Line de-energization may cause stress on the opening CB due to the from 50 Hz differing resonant frequency on the line side depending on compensation degree. Another issue to consider is the thermal stress on the line-side inductive VTs due to relatively high charging reactive power of cable and OHL sections. Worst case will be without shunt compensation of the upper circuit between S/S A and B in Fig. 1. When that circuit is disconnected, three VT sets along the line will be stressed equally and forced to be saturated. The primary current and energy absorption of the VTs for three phases installed near to the shunt reactor are shown in Fig. 17 and Fig. 18, respectively. Maximum energy per VT is 169 kJ.

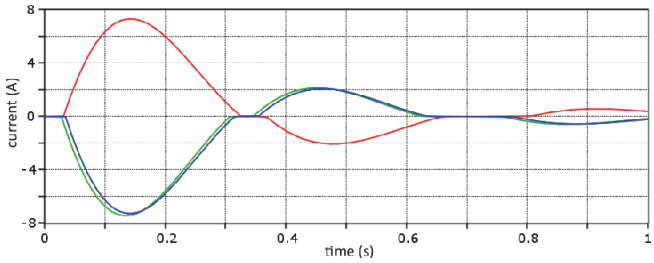


Fig. 17. Current of VTs for three phases at the shunt reactor

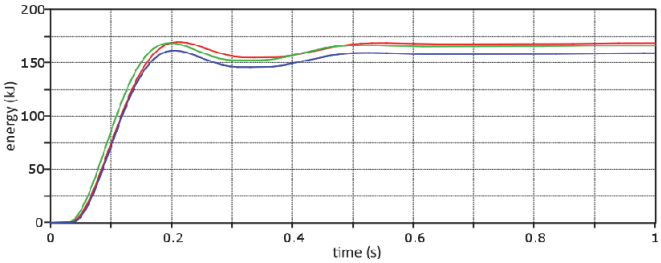


Fig. 18. Energy absorption of VTs for three phases at the shunt reactor

## IV. Conclusions

The paper addressed the most important issues regarding mixed transmission lines consisting of several OHL and cable sections. Due to relatively longer length of cable sections reactive power compensation by a shunt reactor connected to each circuit of the line with variable power is required. In addition, the cable sections should be protected against lightning overvoltages by surge arresters by installing at each OHL-cable junction. The planned double-circuit 380-kV mixed line has been modelled in detail with the graphical pre-processor ATPDraw to EMTP-ATP. In this paper the focus is put on switching and fault transients of that mixed line, particularly by taking the interaction of the shunt reactor with the line into consideration. Simulation results of line energization show no critical overvoltages and stress on closing circuit breaker. There is no need for controlled switching at voltage zero-crossing. However, the use of pre-insertion resistor CB's improve overvoltage stress on equipment significantly. Due to line-side connected shunt reactor the secondary arc duration is expected to be longer compared to a line without shunt compensation. De-energization simulations are not treated in this paper in detail. Several factors like line loading and compensation degree may cause crucial stress on the opening CB at both ends due to the recovery voltage. Inductive VTs are also stressed by line de-energization.

## References


[1] German federal network agency for electricity, gas, telecommunications, post and railway, Status of the Grid Expansion according to the Law of Transmission Grid Expansion (EnLAG) and Federal Requirements Plan for the 3rd quarter 2016, 30.09.2016 [Online]. Available in German: https://www.netzausbau.de/leitungsvorhaben/de.html

[2] H. Khalilnezhad, S. Chen, M. Popov, J.A. Bos, J.P.W. de Jong, L. van der Sluis, "Shunt Compensation Design of EHV Double-Circuit Mixed OHL-Cable Connections", unpublished. Presented at the IET International Conference on the Resilience of Transmission and Distribution Networks, Birmingham, UK, 2015.

[3] Canadian/American EMTP User Group *ATP Rule Book*, Portland, Oregon/USA, revised and distributed by the EEUG Association (http://www.eeug.org), last revision, 2014.

[4] IEEE Working Group 3.4.11-Surge Protective Devices Committee, "Modeling of Metal Oxide Surge Arresters", *IEEE Trans. on Power Delivery*, Vol. 7, No. 1, pp. 302- 309, January 1992.

[5] P. Pinceti, M. Giannettoni, "A simplified model for zinc oxide surge arresters", *IEEE Transactions on Power Delivery*, Vol. 14, No. 2 pp. 393-398, April 1999.

[6] M. C. Magro, M. Giannettoni, P. Pinceti, "Validation of ZnO Surge Arresters Model for Overvoltage Studies", *IEEE Transactions on Power Delivery*, Vol. 19, No. 4, pp. 1692-1695, October 2004.

[7] A. Mackow, M. Kizilcay, "Transient Studies of Power Cable Sections in a 380-kV Transmission System", unpublished, presented at the 9th International Conference on Insulated Power Cables, Versailles, France, 2015. [Online]. Available: http://www.jicable.org

[8] M. Kizilcay, M. V. Escudero, "Resonant overvoltages on reactor compensated EHV lines due to single- or three-phase line tripping", in *Proc. 2001 European EMTP-ATP Conference*, Bristol, UK.

[9] CIGRE WG C4.502 (W. Wiechowski, Convener). Power System Technical Performance Issues Related to the Application of Long HVAC Cables, CIGRE Brochure, no. 556, Oct. 2013.

[10] CIGRE WG C4.307 (Z. Emin, Convenor). Resonance and Ferroresonance in Power Networks, CIGRE Brochure, no. 569, Feb. 2014.

[11] F. F. da Silva, C. L. Bak, U.S. Gudmundsdottir, W.Wiechowski, M.R. Knardrupgard, "Methods to Minimize Zero-Missing Phenomenon", *IEEE Transactions on Power Delivery*, vol. 25, no. 4, pp.2923-2930, Oct. 2010.

[12] S. Wijesinghe, K.K.M.A. Kariyawasam, B. Jayasekera, D. Muthumuni, M. Chowns, "Transients Following the Energizing of High Voltage AC Cables with Shunt Compensation", unpublished. Presented at Int. Conf. on Power Systems Transients, Vancouver, Canada, 2013. [Online]. Available: http://www.ipstconf.org/Papers.html

[13] M. Kizilcay, G. Bán, L. Prikler, P. Handl, "Interaction of the Secondary Arc with the Transmission System during Single-Phase Autoreclosure", in *Proc. 2003 IEEE Bologna Power Tech Conference*, Bologna, Italy.

[14] M. Kizilcay, P. La Seta, "Digital simulation of fault arcs in medium-voltage distribution networks", in *Proc. 2005 15th Power Systems Computation Conference*, Liège, Belgium.

[15] A.T. Johns, R.K. Aggarwal, Y.H. Song, 1994; "Improved Techniques for Modeling Fault Arcs on Faulted EHV Transmission System", *Proc. 1994 IEE - Generation, Transmission and Distribution*, vol. 141, no. 2, pp.148-154.

[16] J. Luhmann, "Simulation of ferroresonance in HV voltage transformers using EMTP under consideration of hysteresis and eddy currents and their metrological verification", Ruhr-University Bochum, Faculty of Electrical Eng., diploma thesis, 1996 (in German).